Ferromagnetic Behavior of the New Hydride $CeNiSnH_{1.8(2)}$†

B. Chevalier,*,‡ J-L. Bobet,‡ M. Pasturel,‡ E. Bauer,§ F. Weill,‡ R. Decourt,‡ and J. Etourneau‡

Institut de Chimie de la Matière Condensée de Bordeaux (ICMCB), CNRS [UPR 9048], Université Bordeaux 1, Avenue du Docteur A. Schweitzer, 33608 Pessac Cedex, France, and Institut für Festkörperphysik, Technische Universitaet Wien, Wiedner Hauptstrasse 8-10, A-1040 Wien, Austria

Received November 28, 2002. Revised Manuscript Received February 25, 2003

The ternary stannide CeNiSn absorbs hydrogen at 250 °C under a pressure of $P_{H2} = 5$ MPa. The resulting hydride $CeNiSnH_{1.8(2)}$ crystallizes in the hexagonal ZrBeSi-type structure with $a = 0.4392(2)$ nm and $c = 0.8543(2)$ nm as unit cell parameters. Investigation by means of magnetization and electrical resistivity measurements show that (i) $CeNiSnH_{1.8(2)}$ exhibits a ferromagnetic order below $T_C = 7.0(2)$ K and (ii) Kondo scattering dominates the electrical properties. This study points out that hydrogenation of CeNiSn provokes a change of the ground state of cerium, from Kondo insulator to ferromagnetic behavior.

Introduction

Recent work devoted to the hydrogenation of the equiatomic ternary compounds based on cerium CeMX (M = 3, 4, 5d transition element and X = Al, Ga, or In) have shown that their physical properties are strongly modified by the insertion of hydrogen. Among the effects observed are as follows: (i) a valence transition of cerium from intermediate valence to the trivalent state without the occurrence of magnetic ordering down to 2 K for hydrides relative to CeNiAl,[1] CeIrAl,[2] CeNiGa,[3] and CeIrGa;[4] (ii) a strong increase of the magnetic ordering temperature after hydrogenation of CeAuAl[5] and CePtAl;[6] (iii) an interesting transition from intermediate valence to ferromagnetic behavior (CeNiIn); in the latter compound, hydrogenation does not lead to a structural change.[7] These effects result from the expansion of the unit cell volume V_m due to hydrogenation, which increases the magnetic RKKY interaction and decreases the Kondo interaction. The competition between these two interactions explains the physical properties of the intermetallics based on cerium.[8]

The aim of the present work is to study the response of CeNiSn exposed to hydrogen. Ternary stannide CeNiSn does not show magnetic order down to 0.4 K and is characterized as an anisotropic dense Kondo system, forming an energy gap below 12 K.[9] Thus, it is classified as a Kondo semiconductor. It is to be noted that the replacement of Ni by Co, Cu, or Pd in CeNiSn induces a crossover from a nonmagnetic to a magnetic ground state.[10−12] For instance, the unit cell volume V_m of solid solution $CeNi_{1-x}Pd_xSn$ increases with x and antiferromagnetic ordering appears for $x \geq 0.20$.[12] In this view, it is interesting to compare the physical properties of CeNiSn before and after hydrogenation. In this paper, the crystallographic, electrical, and magnetic properties of the new hydride $CeNiSnH_{1.8(2)}$ are reported.

Experimental Details

A polycrystalline CeNiSn sample was synthesized by arc-melting a stoichiometric mixture of pure elements (purity above 99.9%) in a high-purity argon atmosphere. Then, the sample was turned and remelted several times to ensure homogeneity. Annealing was done for 2 weeks at 800 °C by enclosing the sample in evacuated quartz tubes. X-ray powder diffraction confirms that this stannide crystallizes in the orthorhombic ϵ-TiNiSi-type structure (space group $Pn2_1a$) with unit cell parameters $a = 0.7544(2)$ nm, $b = 0.4603(2)$ nm, and $c = 0.7614(2)$ nm (standard deviations in the data of the least-significant digits are given in brackets throughout the paper), in agreement with those reported previously.[13]

Hydrogen absorption experiments were performed using the apparatus described previously.[14] An ingot of an annealed

† PACS Number: 61.10.Nz, 61.14.Lj, 72.15.Eb, 75.50.Ce.

* To whom correspondence should be addressed. Fax: 33-5-56842761. E-mail: chevalie@icmcb.u-bordeaux.fr.

‡ Université Bordeaux 1.

§ Technische Universitaet Wien.

(1) Bobet, J.-L.; Chevalier, B.; Darriet, B.; Nakhl, M.; Weill, F.; Etourneau, J. *J. Alloys Compd.* **2001**, *317−318*, 67.

(2) Malik, S. K.; Raj, P.; Sathyamoorthy, A.; Shashikala, K.; Harish Kumar, N.; Menon, L. *Phys. Rev. B* **2001**, *63*, 172418.

(3) Chevalier, B.; Bobet, J.-L.; Gaudin, E.; Pasturel, M.; Etourneau, J. *J. Solid State Chem.* **2002**, *168*, 28.

(4) Raj, P.; Sathyamoorthy, A.; Shashikala, K.; Venkateswara Rao, C. R.; Malik, S. K. *Solid State Commun.* **2001**, *120*, 375.

(5) Chevalier, B.; Bobet, J.-L.; Kahn, M. L.; Weill, F.; Etourneau, J. *J. Alloys Compd.* **2002**, *334*, 20.

(6) Bobet, J.-L.; Chevalier, B.; Weill, F.; Etourneau, J. *J. Alloys Compd.* **2002**, *330−332*, 373.

(7) Chevalier, B.; Kahn, M. L.; Bobet, J.-L.; Pasturel, M.; Etourneau, J. *J. Phys.: Condens. Matter* **2002**, *14*, L365.

(8) Stewart, G. R. *Rev. Mod. Phys.* **2001**, *73*, 797.

(9) Takabatake, T.; Teshima, F.; Fujii, H.; Nishigori, S.; Suzuki, T.; Fujita, T.; Yamaguchi, Y.; Sakurai, J.; Jaccard, D. *Phys. Rev. B* **1990**, *41*, 9607.

(10) Adroja, D. T.; Echizen, Y.; Takabatake, T.; Matsumoto, Y.; Suzuki, T.; Fujita, T.; Rainford, B. D. *J. Phys.: Condens. Matter* **1999**, *11*, 543.

(11) Echizen, Y.; Umeo, K.; Hamashima, S.; Fujita, T.; Takabatake, T.; Kobayashi, N.; Oguro, I. *Solid State Commun.* **2000**, *115*, 587.

(12) Kasaya, M.; Suzuki, H.; Katoh, K.; Inoue, M.; Yamaguchi, T. Physical Properties of Actinide and Rare Earth Compounds, JJAP Series, **1993**, *8*, 223.

(13) Higashi, I.; Kobayashi, K.; Takabatake, T.; Kasaya, M. *J. Alloys Compd.* **1993**, *193*, 300.

10.1021/cm0213669 CCC: $25.00 © 2003 American Chemical Society
Published on Web 04/17/2003

sample was heated under vacuum at 250 °C for 12 h and then exposed to 5 MPa of hydrogen gas at the same temperature. The amount of H absorbed was determined volumetrically by monitoring pressure changes in a calibrated volume. After synthesis, the hydride sample was kept and manipulated under argon in a dry box.

X-ray powder diffraction with the use of a Philips 1050-diffractometer (Cu Kα radiation) was applied for the characterization of the structural type and for the phase identification of the hydride sample. The unit cell parameters were determined by a least-squares refinement method using silicon (5N) as an internal standard. The crystal structure of the sample obtained by hydrogenation was refined by the Rietveld profile method.[15]

For electron microscopy experiments (JEOL 2000FX), parts of the hydride sample were crushed in ethanol in an agate mortar and the small fragments were placed on a copper grid covered with an amorphous holey carbon film.

Magnetization measurements were performed using a Superconducting Quantum Interference Device (SQUID) magnetometer in the temperature range 1.8−300 K and applied fields up to 5 T. The ac susceptibility was determined without dc magnetic field but with an ac field of 2×10^{-4} T and a frequency of 12.5 Hz. Electrical resistivity was carried out above 4.2 K on a polycrystalline sample using standard dc four-probe measurements. For this investigation, the hydride was compacted at room temperature to form a pellet (diameter = 6 mm and thickness = 3 mm) and then heated for 2 days at 250 °C under pressure (5 MPa) of hydrogen.

Results and Discussion

Under the experimental conditions described above, CeNiSn absorbs hydrogen. The amount of H atom inserted is 1.8(2) per CeNiSn formula. The hydride formed is stable in air. In contrast, after heating at 250 °C under vacuum (1.3×10^{-7} MPa), it decomposes into another hydride, $CeNiSnH_{1.0(2)}$, crystallizing like CeNiSn in an orthorhombic unit cell with $a = 0.7273(3)$ nm, $b = 0.4411(2)$ nm, and $c = 0.8458(3)$ nm as lattice parameters. The crystallographic and physical properties of this last hydride will be reported soon.

The absorption of hydrogen by CeNiSn modifies its structural properties. The X-ray powder pattern of the $CeNiSnH_{1.8(2)}$ hydride is indexed on the basis of a hexagonal unit cell with the ZrBeSi-type structure (space group $P6_3/mmc$; No. 194) (Figure 1). (Some traces of CeO_2 oxide could be detected by X-ray powder diffraction). To confirm this crystal symmetry, we have examined some small crystals of $CeNiSnH_{1.8(2)}$ by transmission electron microscopy. Selected-area electron diffraction patterns along the zone directions [1 −1 0], [0 −1 0], and [0 0 1] are shown in Figure 2. This study reveals hexagonal symmetry of the crystal structure of hydride $CeNiSnH_{1.8(2)}$ (see the pattern along the [0 0 1] direction). Further, the pattern along the [1 −1 0] direction indicates that for (*hhl*) reflections a condition for extinction exists: *hhl* with $l = 2n + 1$. This agrees with the presence of a *c*-type glide plane as for the ZrBeSi-type structure (space group $P6_3/mmc$). The crystallographic parameters (unit cell and atomic coordinates), determined from the Rietveld profile refinement of the X-ray data, are listed in Table 1. After refinement, the values of the reliability factors R_F, R_p, and R_{wp} were 0.065, 0.124, and 0.164, respectively.

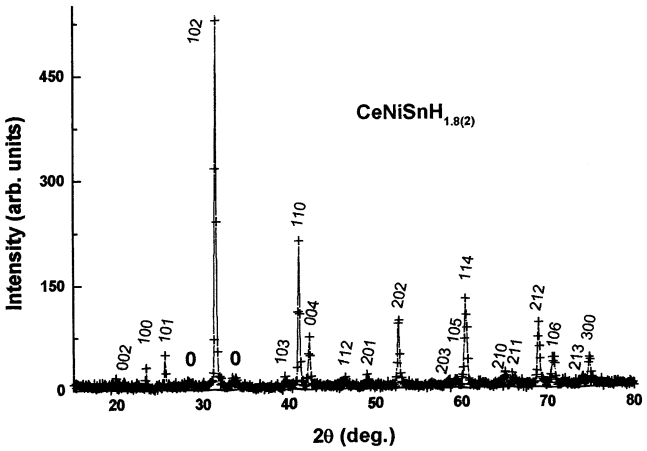

Figure 1. X-ray powder diffraction pattern of $CeNiSnH_{1.8(2)}$ hydride. The Miller indices are relative to the hexagonal unit cell with $a = 0.4392(2)$ nm and $c = 0.8543(2)$ nm. Symbol **0** indicates the peaks ascribed to CeO_2 oxide.

Table 1. Atomic Parameters for $CeNiSnH_{1.8(2)}$ (Space Group $P6_3/mmc$, Unit Cell Parameters $a = 0.4392(2)$ nm and $c = 0.8543(2)$ nm)

atom	site	*x*	*y*	*z*	*B* (nm)^2
Ce	2a	0	0	0	0.0021(1)
Ni	2c	$^1/_3$	$^2/_3$	$^1/_4$	0.0038(2)
Sn	2d	$^1/_3$	$^2/_3$	$^3/_4$	0.0032(2)

Table 2. X-ray Powder Diffraction Data for $CeNiSnH_{1.8(2)}$

hkl	$2\theta_{obs}$ (deg)	d_{obs} (nm)	Int_{obs}
002	20.78	0.4271	2
100	23.37	0.3803	3
101	25.62	0.3474	8
102	31.47	0.2840	100
103	39.50	0.2279	3
110	41.07	0.2196	41
004	42.28	0.2136	17
112	46.46	0.1953	3
200	47.79	0.1902	1
104	48.87	0.1862	1
201	49.03	0.1856	3
202	52.64	0.1737	27
203	58.30	0.1581	2
105	59.24	0.1558	2
114	60.41	0.1531	38
210	64.80	0.1438	2
211	65.82	0.1418	3
212	68.85	0.1362	26
106	70.57	0.1333	14
213	73.77	0.1283	2
300	74.83	0.1268	13

Table 2 summarizes the X-ray powder diffraction data of $CeNiSnH_{1.8(2)}$ hydride.

A similar structural transition from orthorhombic TiNiSi-type structure to hexagonal ZrBeSi-type structure has been observed after hydrogenation (or deuteration) of several equiatomic ternary compounds such as CeIrAl,[2] CeAuAl,[5] CeIrGa,[4] and LaNiSn.[16] In this crystal structure Ce, Ni, and Sn atoms occupy, respectively, the 2a (0 0 0), 2c ($^1/_3$ $^2/_3$ $^1/_4$), and 2d ($^1/_3$ $^2/_3$ $^3/_4$) sites (Table 1). The refinement of the crystal structure of $LaNiSnD_2$ indicates that deuterium atoms are located inside the [La_3Ni] tetrahedral site.[16]

The crystal structures of CeNiSn and $CeNiSnH_{1.8(2)}$ (Figure 3) present some similarities:[5] the cerium three-

(14) Bobet, J.-L.; Pechev, S.; Chevalier, B.; Darriet, B. *J. Alloys Compd.* **1998**, *267*, 136.

(15) Rodriguez-Carvajal, J. Powder diffraction. In *Satellite Meeting of the 15th Congress of IUCr*, Toulouse, 1990; p 127.

(16) Yartys, V. A.; Olavesen, T.; Hauback, B. C.; Fjellvag, H.; Brinks, H. W. *J. Alloys Compd.* **2002**, *330−332*, 141.

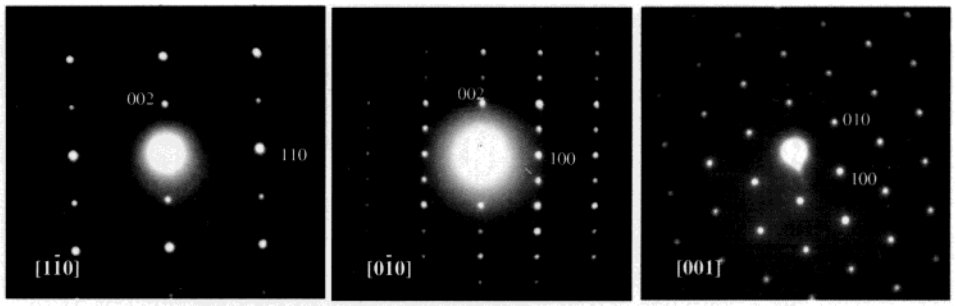

Figure 2. Selected-area electron diffraction patterns of $CeNiSn_{1.8(2)}$ along the [1 −1 0], [0 −1 0], and [0 0 1] direction.

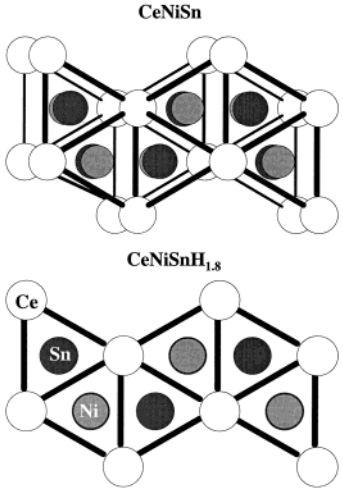

Figure 3. Crystal structure of CeNiSn and $CeNiSnH_{1.8(2)}$ projected respectively onto the (1 0 0) and (0 0 1) planes.

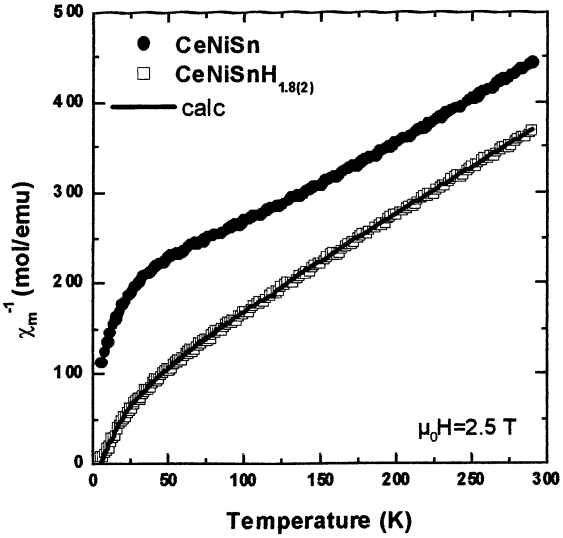

Figure 4. Temperature dependence of the reciprocal magnetic susceptibility, measured with an applied field $\mu_0 H = 2.5$ T, of stannide CeNiSn and its hydride $CeNiSnH_{1.8(2)}$. Solid line shows the fit to calculated χ_m^{-1}, using crystal field effect and molecular field (see text).

dimensional network is described by an intergrowth of trigonal [Ce_6] prisms surrounding alternatively the Ni and Sn atoms. But for CeNiSn, the [Ce_6] prisms are more distorted. Moreover, in these two compounds, Ni and Sn atoms form a hexagonal network which is respectively close-packed and regular in CeNiSn and $CeNiSnH_{1.8(2)}$. Also, the unit cell volume per mole, V_m, increases drastically after hydrogenation from 0.06608[13] to 0.07136 nm^3 (this work). In other words, the volume expansion is equal to 8.0%, very close to that observed (7.85%) upon the deuteration of the ternary stannide LaNiSn.[16]

It is interesting to compare the interatomic distances existing between the Ce atom and its nearest neighbors in both CeNiSn and $CeNiSnH_{1.8(2)}$ (Table 3). The average interatomic distances are clearly shorter in the non-hydrided compound ($d_{Ce-Ni} = 0.3273$ nm and $d_{Ce-Sn} = 0.3268$ nm in CeNiSn and $d_{Ce-Ni} = d_{Ce-Sn} = 0.3315$ nm in $CeNiSnH_{1.8(2)}$). It is well-known that these spacings govern the strength of 4f(Ce)−3d(Ni) or −5p(Sn) interactions responsible for the electronic state of cerium in ternary compounds existing in the Ce−Ni−Sn system.[17] Moreover, the structural transition ϵ-TiNiSi-type (CeNiSn) → ZrBeSi-type ($CeNiSnH_{1.8(2)}$) leads to an increase of the number (6 → 8) of Ce atoms neighboring each other. Finally, the average interatomic distance d_{Ce-Ce} increases from 0.4083 to 0.4362 nm during this structural transition. All these crystallographic data suggest that the electronic ground state of the cerium is strongly modified by insertion of hydrogen in CeNiSn.

Table 3. Selected Interatomic Distances (nm) in CeNiSn[13] and $CeNiSnH_{1.8(2)}$

CeNiSn		$CeNiSnH_{1.8(2)}$	
Ce−Ni	0.3064	Ce−6Ni	0.3315
Ce−Ni	0.3121		
Ce−Ni	0.3135		
Ce−Ni	0.3324		
Ce−Ni	0.3490		
Ce−Ni	0.3503		
Ce−Sn	0.3183	Ce−6Sn	0.3315
Ce−Sn	0.3227		
Ce−Sn	0.3254		
Ce−Sn	0.3285		
Ce−Sn	0.3327		
Ce−Sn	0.3331		
Ce−2Ce	0.37915	Ce−2Ce	0.4272
Ce−2Ce	0.38565	Ce−6Ce	0.4392
Ce−2Ce	0.46009		

As shown in Figure 4, the reciprocal magnetic susceptibility $\chi_m^{-1} = f(T)$ of hydride $CeNiSnH_{1.8(2)}$ is clearly different from that measured for CeNiSn (the data relative to CeNiSn are in agreement with those reported previously by Adroja et al.[18]). The curve $\chi_m^{-1} = f(T)$ of the hydride does not follow a Curie−Weiss law. Deviations from this law are, most likely, related to crystal field effects (CEF). For the hexagonal symmetry, the Ce

(17) Chevalier, B.; Etourneau, J. *J. Mater. Chem.* **1999**, *9*, 1789.

(18) Adroja, D. T.; Rainford, B. D. *J. Magn. Magn. Mater.* **1994**, *135*, 333.

$^2F_{5/2}$ state is split into three doublets: $\Gamma_7 = |\pm^1/_2$, $\Gamma_8 = |\pm^5/_2$, and $\Gamma_9 = |\pm^3/_2$. In the paramagnetic range, the temperature dependence of the reciprocal magnetic susceptibility $\chi_m^{-1} = f(T)$ can be expressed in terms of hexagonal crystal field splitting of the $j = {}^5/_2$ total angular momentum and of molecular field effects, that is,[19,20]

$$\chi_m^{-1} = \chi_{CF}^{-1} - \lambda$$

where χ_{CF} is the susceptibility due to the crystal field effects and λ is the molecular field parameter. For analyses based on data from polycrystalline samples χ_m is given by

$$\chi_m = {}^1/_3\chi_{||} + {}^2/_3\chi_{\perp}$$

where $\chi_{||} = \chi_{CF||}(1 - \lambda_{||}\chi_{CF||})^{-1}$ and $\chi_{\perp} = \chi_{CF\perp}(1 - \lambda_{\perp}\chi_{CF\perp})^{-1}$ are the components of the uniform susceptibility parallel and perpendicular to the *c* axis, respectively. $\chi_{CF||}$ and $\chi_{CF\perp}$ are the respective Van Vleck susceptibilities.[21] Incorporating the CEF Hamiltonian appropriate for $j = {}^5/_2$ and hexagonal systems, that is, $H_{hex} = B_2{}^0O_2{}^0 + B_4{}^0O_4{}^0$ ($B_n{}^m$ are CEF parameters and $O_n{}^m$ are Stevens operators), allows the calculation of $\chi_{CF} = f(T)$ as well as of $\chi_m = f(T)$ by adjusting $B_n{}^m$ and the molecular field parameter $\lambda_{||}$ and $\lambda_{\perp}$. The most satisfying fit to the data (solid line, Figure 4) is then obtained for $B_2{}^0 = {}^{15}/_7$K, $B_4{}^0 = {}^1/_7$ K, $\lambda_{\perp} = -145$ mol/emu, and $\lambda_{||} = 5.5$ mol/emu. This calculation indicates that (i) the doublet $\Gamma_9 = |\pm^3/_2$ is the ground state; (ii) it is separated by 30 and 60 K from the first $\Gamma_7 = |\pm^1/_2$ and the second $\Gamma_8 = |\pm^5/_2$ excited levels, respectively. Note that the ground state doublet is close to both excited states. Since results were used from polycrystalline material, the derived crystal field scheme is only tentative and has to be confirmed by inelastic neutron scattering investigation and specific heat measurements. It is interesting to note that the paramagnetic Curie temperature $\theta_p = 4$ K, estimated from this analysis of the magnetic susceptibility, is positive, suggesting the development of ferromagnetic interactions in this hydride.

Figure 5 presents the thermal dependence of the magnetization of $CeNiSnH_{1.8(2)}$ cooled in an applied field of 0.05 T. The strong increase of the magnetization versus temperature characterizes the occurrence of ferromagnetic ordering. The transition temperature T_C, determined from the inflection point of the magnetization curve $M = f(T)$ equals 7.0(2) K. The existence of spontaneous magnetic ordering of the hydride is confirmed by isothermal magnetization measurements carried out at 2 K (Figure 6). Its magnetization increases strongly at lower applied magnetic fields and then increases slowly. At this temperature, the remanence and the coercitive field are respectively equal to 0.32(5) μ_B/mol and 0.020(5) T, respectively.

The $\Gamma_9 = |\pm^3/_2$ ground state deduced from our analysis of the magnetic susceptibility indicates that, in the ordered magnetic range, the Ce magnetic moment has only a contribution along the *c* axis ($M_{||} = 1.28\ \mu_B$/mol).

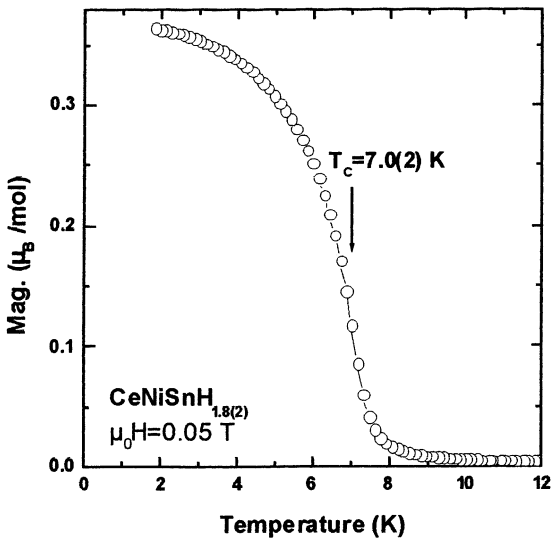

Figure 5. Temperature dependence of the magnetization of the hydride $CeNiSnH_{1.8(2)}$ measured at the applied magnetic field $\mu_0H = 0.05$ T.

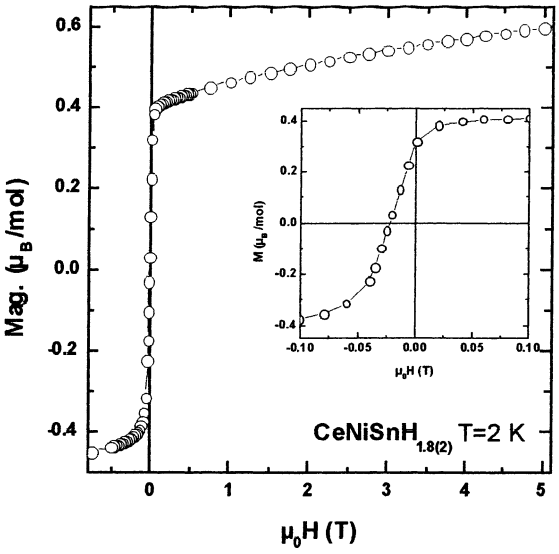

Figure 6. Field dependence at 2 K of the magnetization of the hydride $CeNiSnH_{1.8(2)}$. The inset shows this dependence at low fields.

There is no moment of this state in the basal plane of the hexagonal structure. As the magnetization *M* measurements were performed on polycrystalline $CeNiSnH_{1.8(2)}$ hydride, the resulting value of *M* is given at 0 K by

$$M = {}^1/_3M_{||} + {}^2/_3M_{\perp} = {}^1/_31.28\ \mu_B/\text{mol} = 0.427\ \mu_B/\text{mol}$$

Our study reveals that the spontaneously ordered magnetic moment estimated from the $M = f(\mu_0H)$ curves for $\mu_0H \rightarrow 0$ amounts to about 0.38−0.39 μ_B/mol. This value is smaller than that expected (0.427 μ_B/mol), suggesting the presence of the Kondo effect.

Figure 7 shows the real χ' and imaginary χ'' components of ac susceptibility of $CeNiSnH_{1.8(2)}$. The $\chi' = f(T)$ curve exhibits a strong peak at $T_C = 7.0(2)$ K; this behavior is accompanied at the same temperature by a smaller peak in the $\chi'' = f(T)$ curve. The latter reflects important energy losses in the magnetically ordered

(19) Kitazawa, H.; Schank, C.; Thies, S.; Seidel, B.; Geibel, C.; Steglich, F. *J. Phys. Soc. Jpn.* **1992**, *61*, 1461.
(20) Schröder, A.; Van den Berg, R.; Löhneysen, H. V.; Paul, W.; Lueken, H. *Solid State Commun.* **1988**, *65*, 99.
(21) Segal, E.; Wallace, W. E. *J. Solid State Chem.* **1975**, *13*, 201.

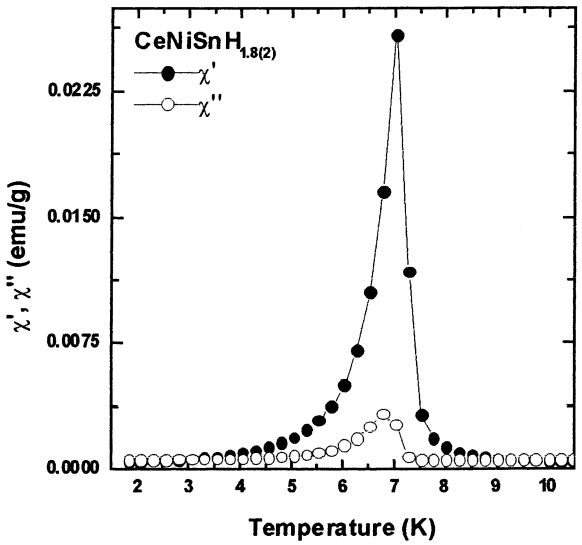

Figure 7. Temperature dependence of the real (χ') and imaginary (χ'') part of the ac magnetic susceptibility of $CeNiSnH_{1.8(2)}$. (ac field = 2×10^{-4} T and frequency = 12.5 Hz)

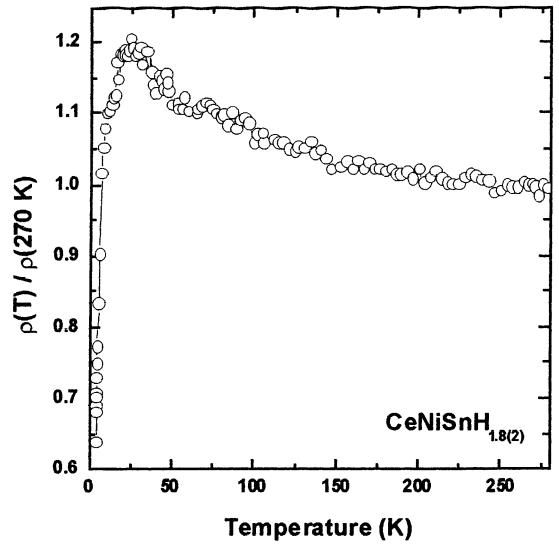

Figure 8. Temperature dependence of the reduced electrical resistivity of hydride $CeNiSnH_{1.8(2)}$.

state and is connected with domain effects appearing, for instance, in ferromagnetic systems.

The influence of the Kondo effect on physical properties of $CeNiSnH_{1.8(2)}$ is clearly evidenced from the thermal dependence of its reduced electrical resistivity (Figure 8). (Due to the presence of microcracks in the polycrystalline sample, the absolute value of ρ could not be determined accurately; for this reason, a reduced representation is chosen). ρ increases in a Kondo-like manner when the temperature decreases from 270 K to about 25 K. At lower temperature, ρ decreases slowly and more rapidly below 7.5(5) K. The latter feature is associated with the occurrence of ferromagnetic ordering of this hydride. Above 25 K, the curve $\rho = f(T)$ is characteristic by incoherent Kondo scattering with a $\rho = -A \log T$ (A = constant) dependence. A similar behavior was observed in other hydrides based on cerium like CeH_{2+x} and is related to the degeneracy of the crystal-field levels.[22]

All the data presented indicate that the hydride $CeNiSnH_{1.8(2)}$ orders ferromagnetically. In other words, the hydrogenation of the stannide CeNiSn drives a transition of the ground state of the cerium atoms from a Kondo semiconductor to magnetically ordered system. This transition can be compared with that observed in the sequence CeNiIn → $CeNiInH_{1.8(1)}$ where the Ce atoms exhibit ferromagnetic ordering for the hydride.[7] To figure out the influence of the Kondo effect on the physical properties of the hydride $CeNiSnH_{1.8(2)}$, specific heat measurements (determination of the electronic coefficient γ and of the magnetic entropy) and neutron powder diffraction (determination of the magnetic moment carried by Ce in the ordered state) are now in progress.

Conclusion

In this paper, it is shown that the hydrogenation of the ternary stannide CeNiSn at 250 °C induces the following: (i) a structural transition from the orthorhombic ϵ-TiNiSi-type structure to the hexagonal ZrBeSi-type structure; (ii) a change of the ground state of the cerium from a Kondo semiconductor to a ferromagnet with $T_C = 7.0(2)$ K. The new hydride $CeNiSnH_{1.8(2)}$ synthesized transforms after heating at 250 °C under vacuum into an another hydride, $CeNiSnH_{1.0(2)}$. Preliminary magnetization measurements performed on the latter evidences antiferromagnetic ordering below $T_N = 4.5(2)$ K. This result suggests that the nature of magnetic ordering appearing in the system $CeNiSnH_X$ is strongly dependent on the H concentration varying the number of the conduction electrons. This value is directly connected to the sign of the magnetic RKKY interactions.

CM0213669

(22) Vajda, P.; Burger, J. P.; Daou, J. N. *Europhys. Lett.* **1990**, *11*, 567.